Journal of Physics: Conference Series

Studying spin diffusion and quantum entanglement with LF-μSR

Journal of Physics: Conference Series **2462** (2023) 012038 doi:10.1088/1742-6596/2462/1/012038

Studying spin diffusion and quantum entanglement with LF-μSR

F L Pratt[1], F Lang[1], S J Blundell[2], W Steinhardt[3], S Haravifard[3], S Mañas-Valero[4], E Coronado[4], B M Huddart[5] and T Lancaster[5]

[1]ISIS Neutron and Muon Source, STFC Rutherford Appleton Laboratory, Chilton, Didcot OX11 0QX, UK
[2]Department of Physics, University of Oxford, Clarendon Laboratory, Oxford OX1 3PU, UK
[3]Department of Physics, Duke University, Durham, North Carolina 27008, USA
[4]Universidad de Valencia (ICMol), Catedrático José Beltrán Martínez, 46980 Paterna, Spain
[5]Department of Physics, Centre for Materials Physics, Durham University, Durham DH1 3LE, UK

E-mail: francis.pratt@stfc.ac.uk

Abstract. LF-μSR studies have previously been used to study the diffusive 1D motion of solitons and polarons in conducting polymers. This type of study was also applied to investigating the diffusive motion of spinons in spin-1/2 antiferromagnetic chains. Recently the method has been extended to examples of 2D layered triangular spin lattices which can support quantum spin liquid states, such as 1T-TaS_2 and $YbZnGaO_4$. These systems are found to show spin dynamics that matches well to 2D spin diffusion, such a model being found to provide a much better fit to the data than previously proposed models for spin correlations in such systems. In $YbZnGaO_4$ the diffusion rate shows a clear crossover between classical and quantum regimes as T falls below the exchange coupling J. That the spin diffusion approach works well in the high T classical region might be expected, but it is found that it also works equally well in the low T quantum region where quantum entanglement controls the spin dynamics. Measurement of the diffusion rate allows a T dependent length scale to be derived from the data that can be assigned to a quantum entanglement length ξ_E. Another entanglement measure, the Quantum Fisher Information F_Q can also be obtained from the data and its T dependence is compared to that of ξ_E.

1. Introduction

LF-μSR studies of low-dimensional electronic spin diffusion originated with conducting polymers, where the muon was used to probe the motion of solitons in trans-polyacetylene [1] and the motion of polarons in polymers such as polyaniline [2, 3] and polyphenylenevinylene [4]. Spin-1/2 antiferromagnetic chains can also support diffusive spin excitations in a certain parameter range of the XXZ model [5, 6] and diffusive models for spin dynamics have been used in μSR investigations of various quantum magnets, including spin chains [7, 8] and spin liquids [9, 10]. Theoretical work has focused mainly on 1D systems and the XXZ model, where diffusive spin transport is expected for exchange anisotropy on the Ising side of the Heisenberg point [5, 6]. With XY anisotropy, the transport has been suggested to switch over to ballistic character [5, 6] and examples of ballistic spin dynamics have also been identified in μSR studies of spin chain systems [11, 12].

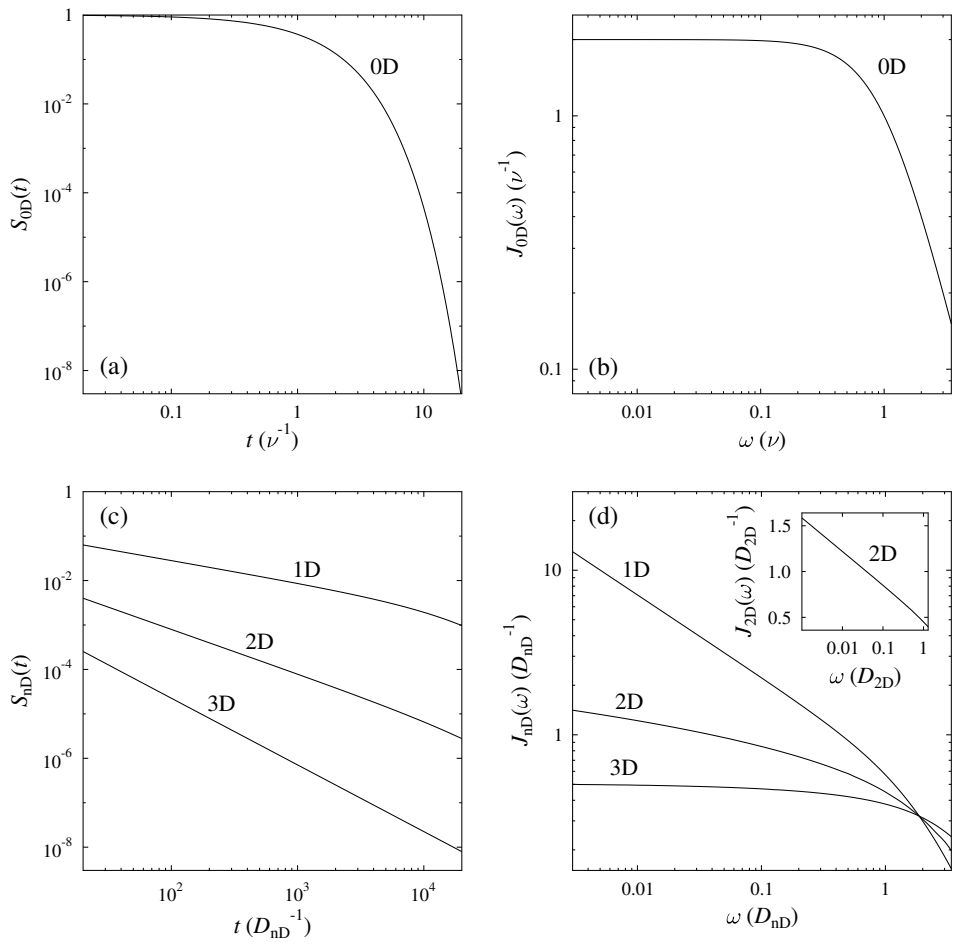

Figure 1. Comparison between the properties of simple localised spin fluctuations and spin fluctuations diffusing on lattices of varying dimensionality. (a) The exponential autocorrelation function for simple localised fluctuations (BPP model) and (b) the corresponding Lorentzian form for the spectral density. (c) The spin autocorrelation function for different types of diffusive processes and (d) their corresponding spectral densities.

The relaxation measured in a LF-μSR experiment can be expressed as being proportional to the spectral density of the spin fluctuations $J(\omega)$ with the probe frequency ω being proportional to the applied field [13]. Depending on the nature of the coupling between the muon and the spin fluctuations, the constant of proportionality between probe frequency and applied field may be either the muon gyromagnetic ratio or the electron gyromagnetic ratio. The spectral density is the Fourier transform of the spin autocorrelation function $S(t)$ and the functions $S(t)$ and $J(\omega)$ are compared in Fig.1 for diffusion on lattices of different dimensions. The case of random fluctuations which are localised and not correlated with those of neighbouring spins can be described by the model of Bloembergen, Purcell and Pound (BPP), also commonly called Redfield theory [13]. This is regarded here as an example of zero dimensional diffusion. The autocorrelation function in this case takes the form

$$S_{0D}(t) = \exp(-\nu t). \tag{1}$$

For diffusion in an anisotropic lattice, the autocorrelation function takes the form [14]

$$S(t) = \prod_{i=1}^{3} \exp(-2D_i t) I_0(2D_i t), \tag{2}$$

where D_i are the diffusion rates in the three different lattice directions and I_0 is a zero order modified Bessel function of the first kind. Where there is uniform fast diffusion in $n = 1$ to 3 dimensions and slow diffusion in the other $3 - n$ dimensions, one can rewrite Eq. 2 as an autocorrelation function reflecting the dominant n-dimensional diffusion

$$S_{\mathrm{nD}}(t) = [\exp(-2D_{\mathrm{nD}}t) I_0(2D_{\mathrm{nD}}t)]^n [\exp(-2D_{\perp}t) I_0(2D_{\perp}t)]^{3-n}, \tag{3}$$

where D_{nD} is the fast diffusion rate and $D_{\perp}$ is the slow diffusion rate. The spectral densities of the 0D to 3D cases all have quite different field dependences (Fig. 1b,d), which allows them in principle to be distinguished in experiment, provided the relaxation rate can be measured over the appropriate field range for the diffusion process.

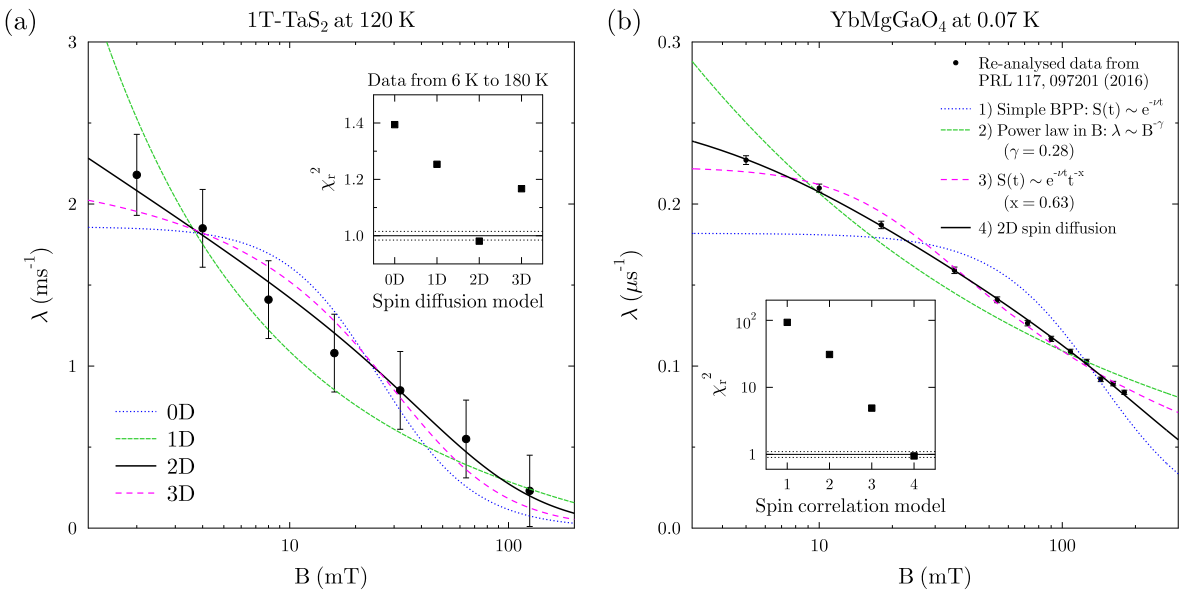

Figure 2. Demonstration that the 2D diffusion model provides the best description of the measured LF-μSR relaxation rates for two different examples of triangular lattice quantum spin liquids. (a) Plot of the LF dependent relaxation rate of 1T-TaS_2 measured at 120 K with fits shown for different dimensionalities of spin diffusion. The 2D model clearly provides the best fit. The inset shows χ^2_r (i.e. χ^2 reduced by normalisation to the number of degrees of freedom) evaluated over fourteen LF scans made at different temperatures. These are plotted versus the dimensionality of the spin diffusion model. The horizontal dashed lines indicate the expected width of the distribution of χ^2_r for a good model description, showing that the 2D model is the only one that falls within this range. (b) A single high statistics LF scan at the base temperature of a dilution fridge was reported by Li *et al.* [15] for $YbMgGaO_4$ and the solid points shown on the plot are obtained from our re-analysis of their raw data. The different lines show best fits for three alternative models, along with the 2D diffusion model. The alternatives however all give much worse fits than the 2D diffusion model and their χ^2_r values are compared in the inset.

2. 2D diffusion in triangular-lattice quantum spin liquids

Recent LF-μSR studies of layered triangular lattice quantum spin liquid (QSL) materials such as 1T-TaS_2 [9] and the pair of isostructural compounds $YbZnGaO_4$/$YbMgGaO_4$ (YZGO/YMGO) have shown spin dynamics that is extremely well described by the 2D spin diffusion model [10], with this model fitting much better than previously proposed models for spin correlations. This is illustrated first in Fig. 2a, where the data points for 1T-TaS_2 [9] are compared against the local fluctuation and spin diffusion models summarised in Fig. 1. That the 2D model is optimum is shown by both the individual LF scan shown in the main plot and the χ^2_r values from combined analysis of data between 6 K and 180 K are shown in the inset.

In the case of YMGO a high statistics LF scan was previously reported by Li *et al.* [15] at 70 mK. The data from this measurement allows a detailed comparison to be made against different models for the spin fluctuations. For consistency of approach, we have re-analysed their raw data, fitting to a stretched exponential with optimal exponent 0.635. The relaxation rate we obtain is plotted as the points in Fig. 2b. The field dependence of the relaxation rate we obtain is then tested against several different models that have been proposed for the spin fluctuations [10] (Fig. 2b). Model 1 is the simple localised fluctuation model expressed by the BPP/Redfield formula based on Eq. 1. Model 2 is a simple power law in field, as used by Majumder *et al.* [16] to fit their data. We obtain the power law 0.28, which is consistent with the value of order 0.3 reported by Majumder *et al.* [16]. Model 3 is based on an approach first used for spin glasses [17] and describes $S(t)$ as the product of an exponential and a power law. This model was presented by Li *et al.* [15] as the best description of their data. We obtain the power law 0.63(1) for this model, which is fully consistent with the value 0.66(5) reported by Li *et al.* in their analysis [15]. Model 4 representing 2D diffusion (Eq. 3 with $n = 2$) is shown as the final model for comparison with the others. The inset plot shows the χ^2_r values for the four different model fits on a log scale, which clearly demonstrates that the 2D spin diffusion model for spin correlations is the only acceptable representation of this data out of these proposed models. A component of the relaxation rate following the characteristic field dependence of 2D diffusion was also found in the analysis of LF-μSR data for YZGO [10] and the properties of this component will be discussed in more detail in section 4.

3. Low energy excitations of the QSL states in 1T-TaS_2 and YZGO

The two QSL systems 1T-TaS_2 and YMGO/YZGO were presented in the previous section as having low energy spin excitations that are well described by a 2D diffusion model. We discuss here the origin of the gapless character of these excitations and their apparent robustness in YZGO/YMGO, even in the presence of short range disorder of the non-magnetic metal atom sites that is a key property of this system. This is illustrated in Fig. 3. The standard resonating valence bond (RVB) picture for the QSL in a triangular lattice (Fig. 3a) involves a ground state that is the superposition of many tilings of short-ranged valence bonds. For YZGO and YMGO the random disorder of the Ga and Mg/Zn sites leads to two different values for the nearest neighbour coupling strength due to different Yb-O-Yb bond angles. The RVB ground state is now a superposition of the subset of tiling states that just include the stronger couplings (Fig. 3b). Although the degeneracy is reduced compared to that of the non-disordered case, the essential character of the RVB state is expected to be retained. The experimental picture for 1T-TaS_2 and YMGO/YZGO is that they are effectively gapless QSL states (any gap, if present, must be small compared to the minimum experimental T). In this case the RVB picture can be modified to reflect much weaker long-ranged valence bonds (Fig. 3c). Such states are expected to be even less susceptible to the effects of short-ranged non-magnetic site disorder than the short-ranged RVB state would be.

The character of QSL states can also be described by the spinon dispersion spectrum calculated via an appropriate mean-field Hamiltonian and defined over the Brillouin zone of

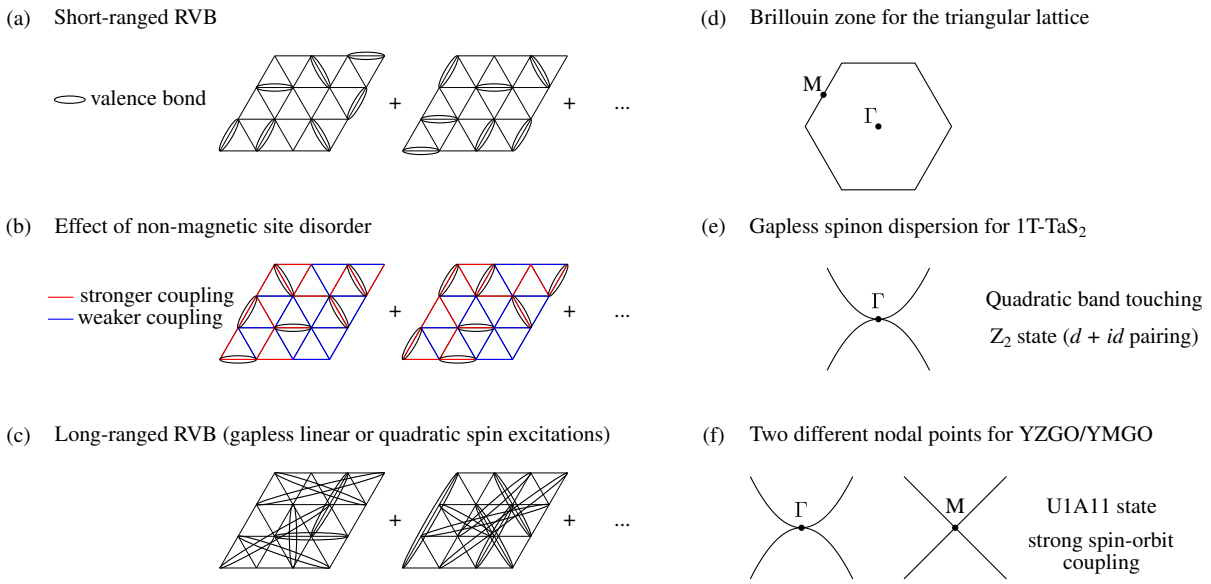

Figure 3. (a) Picture of the the RVB ground state for a triangular lattice. (b) Effect of non-magnetic site disorder in YZGO and YMGO. (c) The RVB model can be extended to weaker long-ranged valence bonds to account for the gapless QSL states found in many experiments. An alternative picture of the QSL state is provided by the spinon dispersion, which is calculated over (d) the Brillouin zone of the triangular lattice. (e) For 1T-TaS_2 a Z_2 paired spinon state with quadratic band touching at the Γ point [18] was suggested to be the ground state [9]. (f) For YZMO/YMGO a predicted U(1) state with two different nodal points [19] was found to be consistent with experiment [10].

the triangular lattice (Fig. 3d). In the case of 1T-TaS_2 a gapless paired spinon state with quadratic band touching at the Γ point was suggested to be the ground state [9] (Fig. 3e). Such a Z_2 QSL state with $d+id$ spinon pairing was found to be stable within the weak Mott insulator parameter range of the Mott-Hubbard model in a variational study by Mishmash *et al.* [18]. For YZGO/YMGO a theoretical study taking into account the the strong spin-orbit coupling leads to three possible U(1) states for the QSL [19]. One of these states, labeled U1A11, has a particular type of dispersion with regions showing both quadratic and linear dispersion around gapless points in the spectrum (Fig. 3f). The gapless regions in the dispersion are point nodes located at the Γ and M points in the Brillouin zone (Fig. 3d). The predicted properties of this U1A11 state were found to match well with a range of experimental results [10].

4. Crossover and entanglement

In YZGO the 2D spin diffusion rate [10] shows a clear crossover between classical and quantum regimes as T falls below the exchange coupling J (Fig. 4a). For the classical paramagnetic region where T is above the characteristic scale defined by J the fluctuations reflect single uncorrelated spin flips, whereas for T below J the cooperative nature of the spin fluctuations sets in. That the spin diffusion approach works well in the high T classical region might be expected, but the measurements also show that it works equally well in the low T quantum region. The right hand side of Fig. 4 compares the diffusion processes in the two regions. In the high T classical region the spin diffusion follows a random walk process with the mean free path being a, the distance between nearest neighbour magnetic sites. The hopping rate is determined by the exchange frequency corresponding to the nearest neighbour coupling. For the low T quantum region the

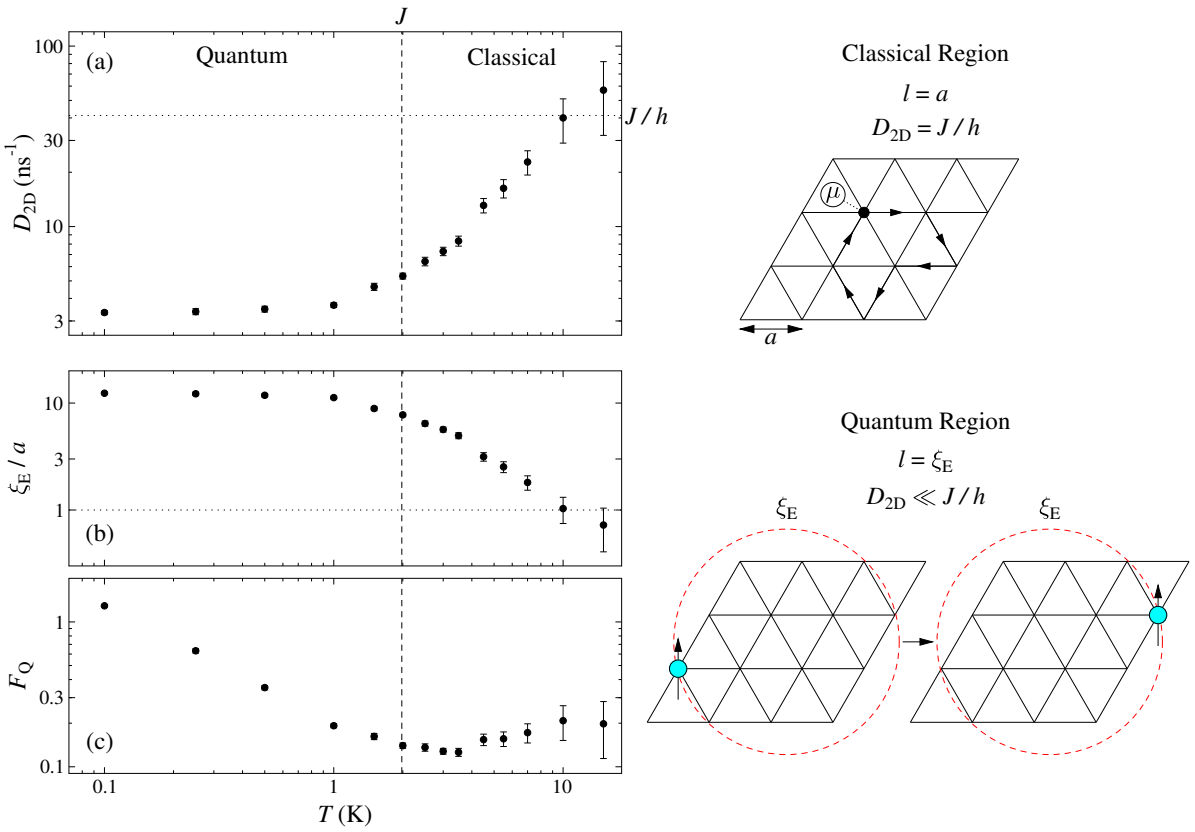

Figure 4. (a) The 2D spin diffusion rate in YZGO [10] showing crossover between quantum and classical regimes around $J = 2.0(2)$ K. The 10 K and 15 K points are consistent with the inverse time scale defined by J/h (horizontal dotted line). (b) The quantum entanglement length ξ_E obtained from Eq. 4. (c) The F_Q values derived by applying Eq. 6 to the fitted $J_{2D}(\omega)$. The right hand side of the figure compares the diffusion processes in the two regions. In the high T classical region the spin diffusion follows a random walk process with the mean free path being a, the distance between nearest neighbour magnetic sites and hopping rate determined by the exchange frequency corresponding to the nearest neighbour coupling. In the low T quantum region the diffusion process for an unpaired spin is expected to have an effective mean free path of the same order as the quantum entanglement length.

spins are highly entangled and the motion of a free spinon requires reorganisation of all the spins within the entanglement region, producing a diffusion process with an effective mean free path on the same order as the entanglement length and leading to a diffusion rate that is much lower than the nearest neighbour exchange frequency that governs the classical diffusion region.

The high velocity spinons expected to dominate the spin transport are those at the M points having linear dispersion (Fig. 3f). These have T independent velocity which leads to the measured diffusion rate being inversely proportional to the mean free path, which can in turn be associated with the entanglement length ξ_E in the quantum region. Hence an estimate of the entanglement length can be obtained, as shown in Fig. 4b [10], given by the inverse of D_{2D}, normalised to the high T classical behaviour, i.e.

$$\xi_E/a = (J/h)/D_{2D}. \tag{4}$$

An alternative approach to estimating entanglement is given by the Quantum Fisher Information metric, F_{Q}, that can be expressed in terms of the imaginary part of the dynamical magnetic susceptibility as [20]

$$F_{\mathrm{Q}} = \frac{4}{\pi}\int_0^{\infty} \tanh\left(\frac{\hbar\omega}{2k_{\mathrm{B}}T}\right)\chi''(\omega,T)d\omega. \tag{5}$$

Using the fluctuation-dissipation theorem this can be expressed in terms of the spectral density function measured by the muon probe

$$F_{\mathrm{Q}} = \frac{4}{\pi}\int_0^{\infty} \tanh^2\left(\frac{\hbar\omega}{2k_{\mathrm{B}}T}\right)J_{2\mathrm{D}}(\omega)d\omega. \tag{6}$$

The spectral density function $J_{2\mathrm{D}}(\omega)$ fitted to the data can be used to extrapolate and evaluate this infinite integral and produce the T dependence of F_{Q} shown in Fig. 4c. In comparison to ξ_{E}, F_{Q} is found to fall off more rapidly with increasing T, becoming very small by the time the exchange coupling J is reached. On the other hand ξ_{E} remains large over the whole of the quantum region and only falls for T significantly above J. One reason for the difference may be that ξ_{E} is derived directly from diffusion, an inherently non-local process, whereas it has been argued that F_{Q} should only be sensitive to local entanglement [20]. Our F_{Q} was however derived from a diffusive spectral density function, so this argument may not be valid here. In any case, it is clear that further work on a range of quantum magnets is needed to gain a better understanding of how these two alternative entanglement measures reflect the properties of such systems.

5. Conclusion

Spin diffusion in 2D layered spin systems is found to provide a good description of the field dependent relaxation in LF-μSR studies. Such a description is a natural extension of the 1D diffusion models previously used to describe the dynamics of solitons and polarons in conducting polymers and spinons in Heisenberg spin chains. For the triangular lattice QSL system 1T-TaS_2, even though the relaxation rate is low, the 2D diffusion model emerges clearly from a global analysis of the LF-μSR data as the best description of the data. In the case of YZGO and YMGO the 2D diffusion model is also shown to provide an excellent description of the LF-μSR. A detailed study of the diffusion rate versus T in YZGO enabled us to observe a crossover at $J = 2$ K between a low T quantum region and a high T classical region. The relatively low value of the exchange coupling J is an important factor here in enabling us to see this fundamental crossover so clearly. A temperature dependent mean free path for the spin diffusion was extracted from the data and assigned to the quantum entanglement length ξ_{E}, a property that becomes significantly enlarged in the quantum region. Derivation of the Quantum Fisher Information from the muon data was also explored as an alternative measure of quantum entanglement in this type of system, producing a noticeably different result for the T dependence of entanglement from that given by ξ_{E} and raising some questions about the interpretation of these different measures. This suggests that, although our studies indicate that there are interesting possibilities for studying quantum entanglement via LF-μSR, further work will be required to fully understand and refine the process of extracting information about quantum entanglement from such muon data.

Acknowledgments
Part of this work was carried out at the ISIS Neutron and Muon Source, STFC Rutherford Appleton Laboratory, U.K. Support was provided by UK EPSRC grants EP/N024028/1, EP/N023803/1 and EP/N024486/1. The work at Duke University has been supported by William M. Fairbank Chair in Physics and NSF under Grant No. DMR-1828348. Work at Valencia was supported by the European Commission (COST Action MOLSPIN CA15128 and ERC AdG Mol-2D 788222 to E.C.) and the Spanish MINECO (Project MAT2017-89993-R co-financed by FEDER and the Unit of Excellence "Maria de Maeztu" MDM-2015-0538) and the Generalitat Valenciana (Prometeo Programme). BMH thanks STFC for support via a studentship. SMV thanks the Spanish Government for the doctoral scholarship F.P.U (FPU14/04407).

References

[1] Nagamine K, Ishida K, Matsuzaki T, Nishiyama K, Kuno Y, Yamazaki T and Shirakawa H 1984, *Phys. Rev. Lett.* **53** 1763
[2] Pratt F L, Blundell S J, Hayes W, Nagamine K, Ishida K and Monkman A P 1997 *Phys. Rev. Lett.* **79** 2855
[3] Pratt F L, Blundell S J, Lovett B W, Nagamine K, Ishida K Hayes W Jestädt Th. and Monkman A P 1999 *Synth. Met.* **101** 323
[4] Pratt F L, Blundell S J, Marshall I M, Lancaster T, Husmann A, Steer C, Hayes W, Fischmeister C, Martin R E and Holmes A B 2003 *Physica* B **326** 34
[5] Ljubotina M, Žnidarič M and Prosen T 2017 *Nat. Commun.* **8** 16117
[6] Bertini B, Heidrich-Meisner F, Karrasch C, Prosen T, Steinigeweg R and Žnidarič M 2021 *Rev. Mod. Phys.* **93** 025003
[7] Pratt F L, Blundell S J, Lancaster T, Baines C and Takagi S 2006 *Phys. Rev. Lett.* **96** 247203
[8] Xiao F, Möller J S, Lancaster T, Williams R C, Pratt F L, Blundell S J, Ceresoli D, Barton A M and Manson J L 2015 *Phys. Rev.* B **91** 144417
[9] Mañas-Valero S, Huddart B M, Lancaster T, Coronado E and Pratt F L 2021 *npj Quantum Mater.* **6** 69
[10] Pratt F L, Lang F, Steinhardt W, Haravifard S and Blundell S J 2022 *Phys. Rev.* B **106** L060401
[11] Lancaster T, Baker P J, Pratt F L, Blundell S J, Hayes W and Prabhakaran D 2012 *Phys. Rev.* B **85** 184404
[12] Huddart B M, Gomilšek M, Hicken T J, Pratt F L, Blundell S J, Goddard P A, Kaech S J, Manson J L and Lancaster T 2021 *Phys. Rev.* B **103** L060405
[13] Blundell S J, De Renzi R, Lancaster T and Pratt F L (eds.) 2021 *Muon Spectroscopy: An Introduction* (Oxford: Oxford University Press)
[14] Butler M A, Walker L R and Soos Z G 1976 *J. Chem. Phys.* **64** 3592
[15] Li Y, Adroja D, Biswas P K, Baker P J, Zhang Q, Liu J, Tsirlin A A, Gegenwart P and Zhang Q 2016 *Phys. Rev. Lett.* **117**, 097201
[16] Majumder M, Simutis G, Collings I E, Orain J-C, Dey T, Li Y, Gegenwart P and Tsirlin A A 2020 *Phys. Rev. Res.* **2** 023191
[17] Keren A, Bazalitsky G, Campbell I and Lord J S 2001 *Phys. Rev.* B **64** 054403
[18] Mishmash R V, Garrison J R, Bieri S and Xu C 2013 *Phys. Rev. Lett.* **111** 157203
[19] Li Y-D, Lu Y-M and Chen G 2017 *Phys. Rev.* B **96** 054445
[20] Hauke P, Heyl M, Tagliacozzo L and Zoller P 2016 *Nature Physics* **12** 778